Acta Crystallographica Section F
Structural Biology Communications
ISSN 2053-230X

Crystallization and preliminary X-ray crystallographic analysis of the complex between the N-D1 domain of VCP from *Homo sapiens* and the N domain of OTU1 from *Saccharomyces cerevisiae*

Su Jin Kim and Eunice EunKyeong Kim*

Biomedical Research Institute, Korea Institute of Science and Technology, Seoul 136-791, Republic of Korea

Correspondence e-mail: eunice@kist.re.kr

Received 27 March 2014
Accepted 7 June 2014

VCP (valosin-containing protein; also known as p97) plays important roles in many biological processes including the ERAD (endoplasmic reticulum-associated degradation) pathway and its function is governed by binding partners. OTU1 (ovarian tumour domain-containing protein 1) is a recently discovered deubiquitinating enzyme that interacts directly with VCP in the ERAD pathway. In order to understand the interactions between the two proteins, the N-D1 domain of VCP and the UBXL domain of OTU1 were cloned, overexpressed, purified and crystallized. The crystals of the complex diffracted to 3.25 Å resolution and belonged to space group $P2_1$, with unit-cell parameters a = 165.45, b = 176.73, c = 165.59 Å, β = 120.095°. There are two molecules of the complex in the asymmetric unit with a Matthews coefficient of 2.62 Å^3 Da^{-1} and a solvent content of 53%.

1. Introduction

VCP (valosin-containing protein; also known as p97 in human and CDC48 in yeast) is an essential and highly abundant AAA+ (ATPase associated with various cellular activities) ATPase. It is conserved from archaea to mammals and participates in many cellular activities such as cell-cycle progression, autophagy, homotypic membrane fusion, transcriptional activation, DNA damage repair, apoptosis, endosomal sorting and regulation of protein degradation at the ER (endoplasmic reticulum) and mitochondrial membrane (Wang *et al.*, 2004; Meyer *et al.*, 2012 and references therein). Dysfunction of VCP is linked to a number of diseases, including cancer, diabetes, inflammation, muscle atrophy and neurodegenerative disorders (Meyer *et al.*, 2012; Yamanaka *et al.*, 2012). VCP consists of an N domain, two ATPase domains called D1 and D2, and a C-terminal tail. It forms a homohexamer using the D1 and D2 domains, and the N domain protrudes from the D1 domain and interacts with binding partners (Pleasure *et al.*, 1993; DeLaBarre & Brunger, 2003). The function of VCP depends on its binding partners. Recently, a number of deubiquitinating enzymes have been associated with VCP in the ERAD (endoplasmic reticulum-associated degradation) pathway (Liu & Ye, 2012); among them, OTU1 (ovarian tumour domain-containing protein 1) is particularly involved in dislocation of substrate from the ER to the cytosol in the ERAD pathway (Ernst *et al.*, 2009). OTU1 consists of a UBXL domain, an OTU domain and a C-terminal zinc finger (Rumpf & Jentsch, 2006; Ernst *et al.*, 2009; Kloppsteck *et al.*, 2012).

Recently, we reported that the UBXL domain of OTU1 adopts a ubiquitin-like fold and binds at the interface of two subdomains of the N domain of VCP using the S3/S4 loop from the complex structure of the N domain of VCP and the UBXL domain of OTU1 (Kim *et al.*, 2014). However, our electron-microscopy (EM) results on the

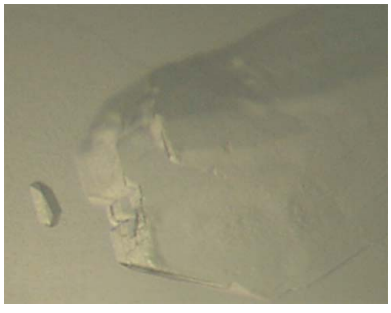

Table 1
Data-collection and processing statistics.

Values in parentheses are for the outermost resolution shell.

Wavelength (Å)	0.97952
Temperature (K)	100
Detector	Q270r
Crystal-to-detector distance (mm)	339.722
Rotation range per image (°)	1
Total rotation range (°)	250
Exposure time per image (s)	5.0
Space group	$P2_1$
Unit-cell parameters (Å, °)	a = 165.453, b = 176.725, c = 165.588, $\alpha = \gamma = 90$, $\beta = 120.095$
Resolution range (Å)	50.00–3.25 (3.37–3.25)
Total No. of reflections	2114441
No. of unique reflections	129420
Completeness (%)	90.5 (80.7)
Multiplicity	16.0
$\langle I/\sigma(I)\rangle$	9.2 (1.8)†
$R_{\rm merge}$‡ (%)	8.9 (24.8)

† The mean $I/\sigma(I)$ falls below 2.0 at 3.37 Å resolution. ‡ $R_{\rm merge} = \sum_{hkl}\sum_i |I_i(hkl) - \langle I(hkl)\rangle| / \sum_{hkl}\sum_i I_i(hkl)$, where $I_i(hkl)$ is the intensity of the unique reflection hkl and $\langle I(hkl)\rangle$ is the average over symmetry-related observations of the unique reflection hkl.

full-length proteins show that only one OTU1 binds to a VCP hexamer. Recent EM studies show that the stoichiometry is 1:1 in the hexameric VCP and UFD1–NPL4 complex while it is 1:1 or 1:3 in the hexameric VCP and FAF1 complex (Bebeacua *et al.*, 2012; Lee *et al.*, 2013; Ewens *et al.*, 2014). This suggests that the binding partner determines the binding ratio and probably induces changes in the structure of VCP. In order to understand how these structural changes translate into biological function, we have investigated the complex structures of hexameric VCP and binding partners. Here, we report the purification and crystallization of the N-D1 domain of VCP in complex with the N domain of OTU1.

2. Materials and methods

2.1. Cloning, expression and purification

The VCP N-D1 domain (VCP ND1; residues 1–458; UniProt accession No. P55072) and the OTU1 UBXL domain (OTU1 N; residues 1–73; UniProt accession No. P43558) were cloned separately into the pET-28a(+) expression vector (Novagen) using the *Bam*HI/*Xho*I restriction sites. The vector contains a hexahistidine tag followed by a thrombin site at the N-terminus. The sequenced plasmids were transformed into the expression host *Escherichia coli* Rosetta (DE3) (Novagen) competent cells. A fresh single colony was picked from the selection on a chloramphenicol/kanamycin plate. Cultures in Luria–Bertani medium were grown to an OD_{600} of 0.6 at 310 K and induced with a final concentration of 500 µ*M* isopropyl β-D-1-thiogalactopyranoside (IPTG) at 291 K.

The two proteins were purified separately in the same manner. The cell pellet was resuspended in buffer *A* (20 m*M* Tris–HCl, 100 m*M* NaCl, 0.5 m*M* TCEP pH 8.0) with 1 m*M* phenylmethylsulfonyl fluoride (PMSF). After sonication, the crude cell extract was centrifuged at 16 000 rev min^{-1} for 30 min at 277 K (A50S-8 rotor). The supernatant was filtered through a sterile 0.45 µm membrane (Sartorius) and then loaded onto an Ni–NTA column (GE Healthcare) previously equilibrated in buffer *A*. The Ni–NTA column was washed with 30 ml buffer *A* containing 20 m*M* imidazole after the sample had been fully loaded. A linear gradient of 20–500 m*M* imidazole in 60 ml was applied. The protein eluted broadly from 50 to 200 m*M* imidazole. After Ni–NTA affinity chromatography, the fractions containing the corresponding protein were concentrated to about 5 ml using a 10 kDa cutoff filter (Sartorius) and loaded onto a HiLoad Superdex 200 26/60 column (GE Healthcare) in buffer *A*. Purified VCP ND1 and OTU1 N formed a complex on mixing the two proteins at a 1:1 molar ratio for 30 min at 277 K after adding 1 m*M* ATP and 2 m*M* magnesium chloride to hexameric VCP ND1. The mixture was concentrated to about 5 ml using a 10 kDa cutoff filter (Sartorius), loaded onto a HiLoad Superdex 200 26/60 column and eluted with buffer *A*. Elution fractions were analyzed for complexes by SDS–PAGE with Coomassie Brilliant Blue staining. The complex of VCP ND1 and OTU1 N was concentrated to about 27 mg ml^{-1}, as estimated by the method of Bradford (1976), prior to crystallization.

2.2. Crystallization

The conditions obtained from initial screening using a Hydra II Plus One (Matrix Technology) robotics system were optimized using the hanging-drop vapour-diffusion method in 24-well plates at 295 K by mixing equal volumes of protein and reservoir solutions and equilibrating against 0.5 ml reservoir solution. Preliminary crystals were obtained from the condition 7%(*w*/*v*) PEG 4000, 600 m*M* NaCl, 100 m*M* PIPES pH 7.0. The crystallization condition was optimized by varying the precipitant gradient, the NaCl concentration and the buffer composition (pH range 6.0–7.5). The best crystals were obtained from a condition consisting of 5%(*w*/*v*) PEG 4000, 450 m*M* NaCl, 100 m*M* PIPES pH 7.0.

2.3. Data collection and processing

Crystals were transferred into a cryoprotectant solution containing 30%(*v*/*v*) ethylene glycol. A single crystal was mounted in a loop and flash-cooled in a nitrogen-gas stream at 100 K. X-ray diffraction data were collected on beamline 7A at the Pohang Light Source (PLS) using an ADSC Quantum Q270r detector with radiation of wavelength 0.97952 Å. The data set was processed, merged and scaled with *HKL*-2000 (Otwinowski & Minor, 1997; Table 1).

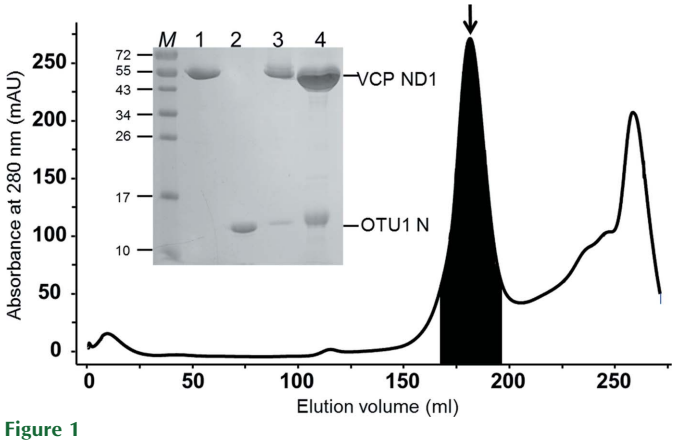

Figure 1
Purification profile and SDS–PAGE analysis of the complex of VCP ND1 and OTU1 N. The arrow represents the major peak. Lane *M*, molecular-mass markers (labelled on the left in kDa); lane 1, VCP ND1; lane 2, OTU1 N; lane 3, protein pooled from the major peak; lane 4, crystal dissolved in buffer *A*.

3. Results and discussion

VCP ND1 and OTU1 N were expressed and purified separately. After formation of the complex of hexameric VCP ND1 and OTU1 N at a 1:1 molar ratio, it was further purified using gel-filtration chromatography and the complex of VCP ND1 and OTU1 N showed a

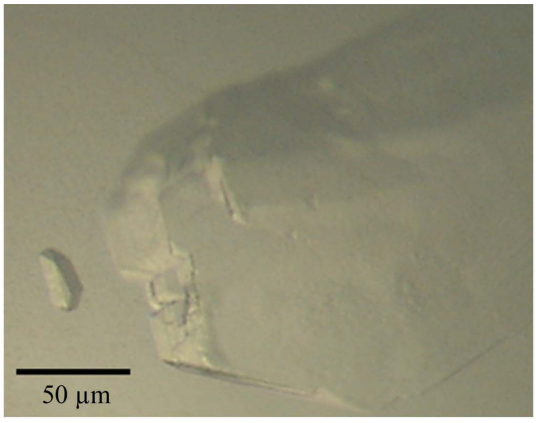

(*a*)

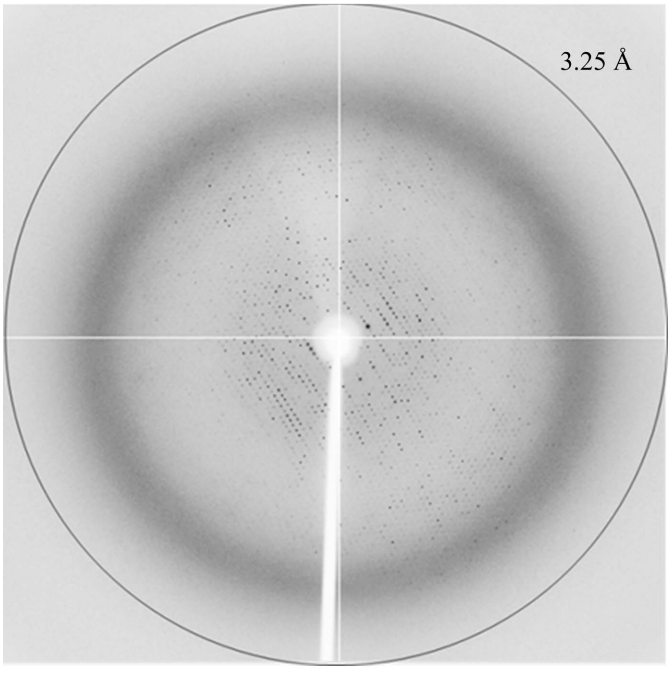

(*b*)

Figure 2
Crystal of the complex of VCP ND1 and OTU1 N and diffraction pattern. (*a*) Complex crystal of VCP ND1 and OTU1 N grown from 5%(*w*/*v*) PEG 4000, 450 m*M* NaCl, 100 m*M* PIPES pH 7.0. (*b*) A diffraction image collected from the crystal. For each frame, the oscillation width and the exposure time were 1° and 5 s, respectively. The high-resolution limit is marked on the figure and the respective value is reported in Å in the top right corner.

major peak at around 181 ml (Fig. 1). SDS–PAGE showed the purity of the complex of VCP ND1 and OTU1 N to be >95%, and the calculated molecular weights were approximately 50 and 15 kDa, respectively (Fig. 1).

The complex of VCP ND1 and OTU1 N was initially crystallized in condition No. 17 of NR-LBD (Molecular Dimensions) [7%(*w*/*v*) PEG 4000, 600 m*M* NaCl, 100 m*M* PIPES pH 7.0]. Diffraction-quality crystals were obtained by equilibrating 1 µl protein solution and 1 µl reservoir solution using hanging-drop vapour diffusion with a reservoir solution consisting of 5%(*w*/*v*) PEG 4000, 450 m*M* NaCl, 100 m*M* PIPES pH 7.0 (Fig. 2*a*). Crystals that were washed three times and dissolved in reservoir solution were verified by SDS–PAGE. This showed that the crystals were definitely formed of the complex of VCP ND1 and OTU1 N (Fig. 1). Unfortunately, many of the crystals were nonmerohedrally twinned and the diffraction could not be easily resolved. A few single crystals were produced by optimization, and we succeeded in collecting a usable data set. The crystal diffracted to 3.25 Å resolution on beamline 7A at the PLS, Republic of Korea (Fig. 2*b*). The crystal appeared to belong to the primitive monoclinic space group $P2_1$, with unit-cell parameters a = 165.45, b = 176.73, c = 165.59 Å, β = 120.095°. The diffraction data set contained 129 420 unique reflections and was 90.5% complete, with an $R_{\rm merge}$ of 8.9%. Table 1 summarizes the statistics of the data collection. The Matthews coefficient ($V_{\rm M}$) was 2.62 Å^3 Da^{-1} with two molecules of the complex of VCP ND1 and OTU1 N in the asymmetric unit, corresponding to a solvent content of 53%, as estimated by the *CCP*4 program *MATTHEWS_COEF* (Matthews, 1968; Winn *et al.*, 2011).

We successfully purified and crystallized the complex of VCP ND1 and OTU1 N. Structure determination by molecular replacement, using the known structures of VCP and OTU1, and refinement are in progress. We expect this structure to provide detailed information on this biologically relevant structure.

We thank the staff of Pohang Light Source beamline 7A. This work was supported by grants from the Global Research Laboratory (GRL) program of the Ministry of Science, ICT and Future Planning of Korea (grant No. 2013056409) and the Institutional Grant from Korea Institute of Science and Technology.

References

Bebeacua, C., Förster, A., McKeown, C., Meyer, H. H., Zhang, X. & Freemont, P. S. (2012). *Proc. Natl Acad. Sci. USA*, **109**, 1098–1103.
Bradford, M. M. (1976). *Anal. Biochem.* **72**, 248–254.
DeLaBarre, B. & Brunger, A. T. (2003). *Nature Struct. Biol.* **10**, 856–863.
Ernst, R., Mueller, B., Ploegh, H. L. & Schlieker, C. (2009). *Mol. Cell*, **36**, 28–38.
Ewens, C. A., Panico, S., Kloppsteck, P., McKeown, C., Ebong, I. O., Robinson, C., Zhang, X. & Freemont, P. S. (2014). *J. Biol. Chem.* **289**, 12077–12084.
Kim, S. J., Cho, J. H., Song, E. J., Kim, S. J., Kim, H. M., Lee, K. E., Suh, S. W. & Kim, E. E. (2014). *J. Biol. Chem.* **289**, 12264–12274.
Kloppsteck, P., Ewens, C. A., Förster, A., Zhang, X. & Freemont, P. S. (2012). *Biochim. Biophys. Acta*, **1823**, 125–129.
Lee, J.-J., Park, J. K., Jeong, J., Jeon, H., Yoon, J.-B., Kim, E. E. & Lee, K.-J. (2013). *J. Biol. Chem.* **288**, 6998–7011.
Liu, Y. & Ye, Y. (2012). *Curr. Protein Pept. Sci.* **13**, 436–446.
Matthews, B. W. (1968). *J. Mol. Biol.* **33**, 491–497.
Meyer, H., Bug, M. & Bremer, S. (2012). *Nature Cell Biol.* **14**, 117–123.
Otwinowski, Z. & Minor, W. (1997). *Methods Enzymol.* **276**, 307–326.
Pleasure, I. T., Black, M. M. & Keen, J. H. (1993). *Nature (London)*, **365**, 459–462.
Rumpf, S. & Jentsch, S. (2006). *Mol. Cell*, **21**, 261–269.
Wang, Q., Song, C. & Li, C.-C. H. (2004). *J. Struct. Biol.* **146**, 44–57.
Winn, M. D. *et al.* (2011). *Acta Cryst.* D**67**, 235–242.
Yamanaka, K., Sasagawa, Y. & Ogura, T. (2012). *Biochim. Biophys. Acta*, **1823**, 130–137.